# Measurement of the Positron-Electron Ratio in the Primary Cosmic Rays from 5 to 50 GeV*

A. Buffington, C. D. Orth, and G. F. Smoot
*Space Sciences Laboratory and Lawrence Berkeley Laboratory, University of California, Berkeley, California 94720*
(Received 9 May 1974)

We report the first measurement of primary-cosmic-ray positrons above 5 GeV. Both $e^+$ and $e^-$ fluxes were measured, using a balloon-borne magnetic spectrometer. Background was suppressed using a new technique which combines both selective trigger and identification of bremsstrahlung photons created by $e^\pm$ upon entering the instrument. If no positrons originate at cosmic-ray sources, our observed ratio $e^+/(e^+ + e^-) = 0.08 \pm 0.02$ requires source protons to traverse $3.5 \pm 1.5$ g/cm$^2$ of interstellar material.

Primary cosmic rays generate secondary cosmic rays through interactions with the interstellar gas. The fluxes of secondaries are a measure of the material traversed by their parents. While secondary nuclei (e.g., Li, Be, B) arise from low-momentum-transfer fragmentation of heavier nuclei, positrons are the decay products of pions produced in highly inelastic proton interactions. As a result, secondary nuclei have the same energy per nucleon as their parents, while positrons have energies typically 5 to 30 times smaller than their parents.

Cosmic-ray nuclei traverse a mean column density which diminishes from about 4 g/cm$^2$ at a few GeV/nucleon to about 2 g/cm$^2$ by 50 GeV/nucleon.[1-5] A measurement of the positron flux above a few GeV provides the means to see if this diminishing trend continues, since these positrons are produced by protons with energies above 50 GeV.

In this Letter we present the first separated $e^+$ and $e^-$ flux measurements in the energy range from 5 to 50 GeV. We used a new technique which combines a radiator to produce bremsstrahlung photons, a superconducting magnetic spectrometer to deflect the incident $e^\pm$, and a multigap lead-plate spark chamber to identify the resulting photon and $e^\pm$ showers. The shower from the bremsstrahlung photons appears in the lead-plate chamber near the extrapolated tangent of the incident $e^\pm$ trajectory, while the shower from the $e^\pm$ appears at the end of its deflected trajectory. Figure 1 is a schematic of the apparatus: more complete details appear elsewhere.[6,7] A good $e^\pm$ event presents a unique topology: a single particle passing through the optically viewed spectrometer spark chambers, and two showers properly located in the lead-plate spark chamber. When combined with an initial background rejection accomplished by triggering with a high threshold on a scintillator located below the lead chamber, this topology requirement reduces the proton and other background to a negligible level. This was verified for 4.5-GeV/$c$ protons from the Lawrence Berkeley Laboratory Bevatron, where calibration of the apparatus gave a rejection of better than $10^{-4}$.

The instrument was flown to an altitude of 35.3 km on a balloon from Palestine, Texas, on the night of 2 November 1972. The events from the flight were scanned to impose the proper $e^\pm$ topology. Events thus selected were measured by hand and analyzed to reconstruct the particle trajectory, determine its energy, and predict the proper shower locations in the lead-plate chamber.[8] The final rejection of background was made by a comparison of the predicted bremsstrahlung-conversion locations with the observed locations. Figure 2 shows a scatter plot of the results. A dense region of correct predictions lies in the middle of the plot, and a small scatter of events

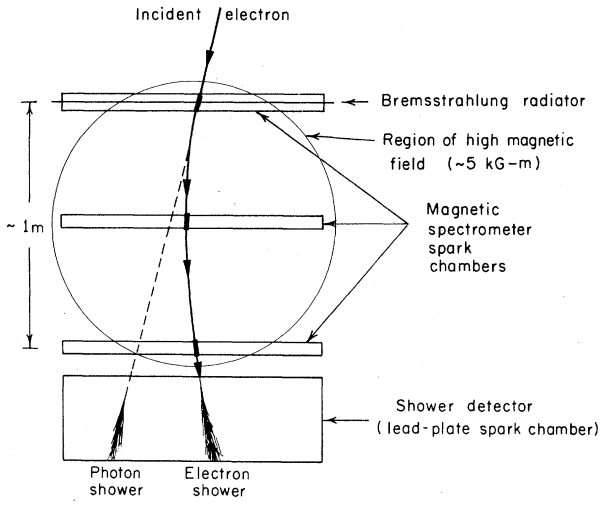


FIG. 1. Schematic diagram for the apparatus.

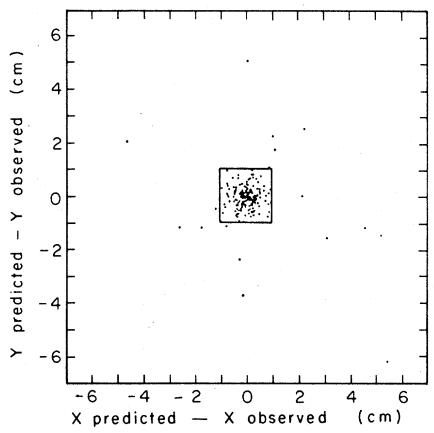


FIG. 2. Comparison of bremsstrahlung-photon real-space location as predicted by the spectrometer measurement, and as actually observed for a portion of our data. We have included only events above 2 GeV in the spectrometer, since multiple Coulomb scattering broadens the distribution below this energy. Events outside of the 2-cm box are rejected as "background."

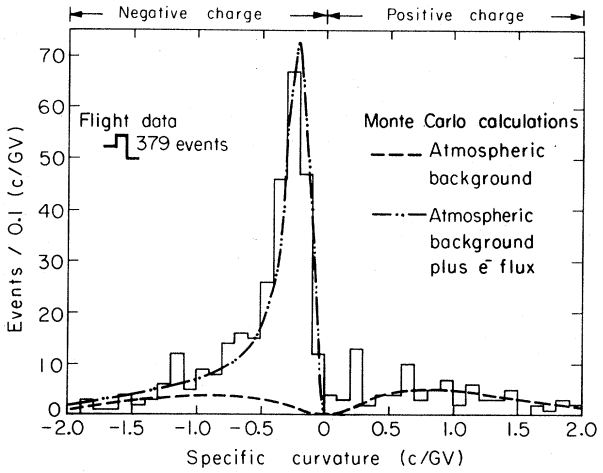


FIG. 3. Specific curvature (inverse momentum per unit charge) distribution for events selected as $e^{\pm}$. Resolution = 0.02 $c$/GV.

with wrong predictions lies away from the center. About two thirds of the events outside the selection box shown are positively charged, presumably proton background. Assuming that such background puts these "bremsstrahlung photon showers" inside the selection box with about the same density as just outside the box, we conclude that no more than one or two of the events inside the box which we call positrons could actually have been protons simulating all criteria for true $e^+$. Similarly, from a study of the distribution of true $e^{\pm}$, we see that no more than 5% of real $e^{\pm}$ could have been lost by imposing the bremsstrahlung-box criterion. In any case, the details of the selection box are not relevant for the ratio $e^+/(e^+ + e^-)$ reported here because the proton background is so low and the $e^{\pm}$ analysis is charge symmetric.

To determine the overall efficiency of the technique for $e^{\pm}$ detection, we made a preflight test at the Stanford Linear Accelerator Center. There we found the efficiency to be 55% for detecting $e^-$ at 5 and 15 GeV. The efficiency was expected to drop slowly to about 25% at 50 GeV, where the two showers in the lead-plate chamber begin to merge and cannot be separately discerned. Efficiency in flight was expected to be slightly reduced by the added gondola material above the spectrometer.

As a cross check of the expected efficiency in flight, we selected as good $e^-$ in a portion of our data all negatively charged events which showered in the lead-plate chamber. The result was 108 good $e^-$ events with properly identified bremsstrahlung showers and 57 good $e^-$ events not meeting the bremsstrahlung-scan criteria. Using a Monte Carlo program simulating the apparatus geometry and the bremsstrahlung radiation process, we predict that these two event categories and the category of $e^-$ events failing the other selection criteria should be in the respective fractions 0.51, 0.32, and 0.17. These figures compare favorably with the scanning results, and therefore verify the efficiency of our technique. Including trigger efficiency, our overall efficiency was 0.47.

After analyzing 77% of our data, representing about 27 min of live time with a geometry factor of $840 \pm 30$ cm$^2$ sr, we found 379 $e^{\pm}$ events. The distribution of these events as a function of specific curvature (the inverse of momentum per unit charge) is shown in Fig. 3. To convert specific curvature to primary energy, one must invert and then scale up by the bremsstrahlung-degradation factor. This factor is energy and spectrum dependent, but is about 1.4 for our data. Scaling is required because the observed energy of an $e^{\pm}$ is not its primary energy, but its energy as degraded by bremsstrahlung in 0.54 radiation length of material above the spectrometer (0.39 from the gondola, 0.15 from the atmosphere). The degradation for an $e^+$ is of course the same as the degradation for an $e^-$.

To obtain primary $e^{\pm}$ fluxes, we must subtract the atmospherically generated flux of $e^{\pm}$ from the

distribution in Fig. 3. This was done using a Monte Carlo program, a proton flux of $dN/dE = 1.9\times10^4 E^{-2.75}/\mathrm{m}^2$ sr sec GeV,[9,10] hadron interaction properties, and an experiment exposure factor. The resulting absolute $e^\pm$ background expected from proton interactions in the 5.6 g/cm$^2$ of atmosphere above the apparatus is shown in Fig. 3 (dashed curve). The falloff in background above $\pm 1$ $c$/GV is due to apparatus trigger threshold. Reentrant albedo is expected to be a small effect, and indeed we see no enhancement of low-energy events.

A subtraction of atmospheric background leaves 267 $e^\pm$ events. Taking the efficiency into account, we estimate an absolute $e^+ + e^-$ flux of $4.2 \pm 0.6$ particles/m$^2$ sr sec above an assumed average geomagnetic cutoff of 4 GV/c. In a future publication, we will analyze the importance of this flux measurement, as well as our study of the spectral indices of the $e^+$ and $e^-$ fluxes. In this Letter, we concentrate on the ratio $e^+/(e^+ + e^-)$.

Proper treatment of the atmospheric background is essential to extract a meaningful ratio $e^+/(e^+ + e^-)$ from our data. Note that the background near zero specific curvature in Fig. 3 is very small. There are two reasons for this. First, because the cosmic-ray spectrum of proton parents is a power law, the atmospheric background vanishes at zero specific curvature (infinite momentum). Second, the time-dilation–inhibited decay of high-energy muons in the atmosphere reduces the background near zero specific curvature even further.

The dot-dashed curve in Fig. 3 is the total expected spectrum derived by adding the atmospheric background and a Monte Carlo prediction for the bremsstrahlung-degraded flux of primary $e^-$. For the primary $e^-$ spectrum, we used $dN/dE \propto E^{-2.83}$ (the 2.83 was obtained by drawing a line through a recent compilation of $e^\pm$ data[11]), and normalized to our observed $e^-$ flux. The fit for the total $e^-$ curve is good, but there is an excess above background near zero specific curvature for positive charge. These events we interpret as the true observed $e^+$ signal originating outside of the atmosphere. We emphasize that this $e^+$ signal could not have resulted from "spillover" from the large $e^-$ peak because the position of the bremsstrahlung shower uniquely determines the charge for each event and our resolution is much less than our bin size. Our rejection of protons is sufficiently strong that proton contamination in the $e^+$ sample could not be more than 10%. An improper assessment of atmospheric background could not possibly account for all of the $e^+$ signal, even though our atmospheric calculation might be in error by as much as 40% at high energies.

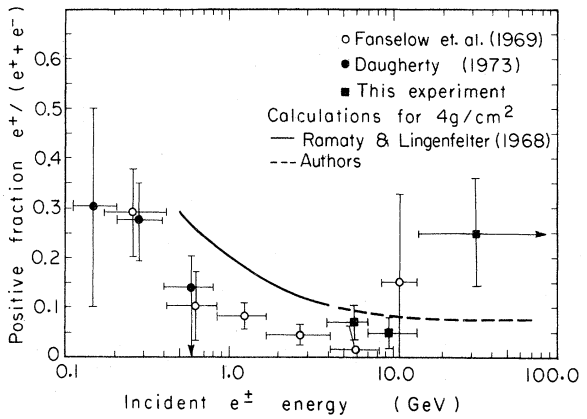


FIG. 4. Ratio $e^+/(e^+ + e^-)$ as a function of incident energy, corrected to top of atmosphere. Smooth curves indicate the expected ratio of $e^+$ production from interactions of cosmic-ray protons and nuclei with the interstellar gas, divided by the total measured $e^+ + e^-$ primary flux.

Figure 4 shows the ratio $e^+/(e^+ + e^-)$ obtained from Fig. 3 and scaled to energy at the top of the atmosphere. Also shown are the previous lower-energy measurements.[12,13] Ratios at higher energies have been inferred from east-west asymmetry measurements,[14,15] but the results are only qualitative.

To determine the mean interstellar column density associated with our results in Fig. 4, we have plotted the expected ratio for 4 g/cm$^2$ based on Ramaty and Lingenfelter's calculation of $e^+$ secondaries,[16] our measured total $e^\pm$ flux, our assumed $e^\pm$ spectral index, and a smooth connection to low-energy data.[12,13] We have also included our own estimate for 4 g/cm$^2$ at higher energies. This calculation could be in error by as much as 40%, partly from uncertainty in the flux of parent protons, and partly from uncertainties in proton interaction dynamics.

We find that our average ratio $e^+/(e^+ + e^-) = 0.08 \pm 0.02$ can be explained by protons of 50 to 1000 GeV having traversed approximately 3.5 $\pm 1.5$ g/cm$^2$ of interstellar material, if no positrons originate at the source of cosmic rays. Considering the uncertainties, we feel that this result is consistent with the $\lesssim 2$ g/cm$^2$ traversed by nuclear cosmic rays, and thus protons and nuclear cosmic rays have probably had the same history. We also feel that there is no significant

evidence for positrons in our energy range coming directly from the sources.

*Work supported by Grant No. NAS 9-7801 from the National Aeronautics and Space Administration and by the Lawrence Berkeley Laboratory.

[1]G. F. Smoot, L. H. Smith, A. Buffington, L. W. Alvarez, and M. A. Wahlig, "Primary Cosmic Ray Nuclear Rigidity Spectra," in Proceedings of the Joint Meeting of the American Physical Society and the American Astronomical Society, San Juan, Puerto Rico, December 1971 (unpublished), and in Information zur Kernforschung und Kerntechnik Zentralstelle Für Atomkernenergie Documentation No. 3 (1972).

[2]E. Juliusson, P. Meyer, and D. Müller, Phys. Rev. Lett. 29, 445 (1972).

[3]J. F. Ormes and V. K. Balasubrahmanyan, Nature (London), Phys. Sci. 241, 95 (1973).

[4]W. R. Webber, J. A. Lezniak, J. C. Kish, and S. V. Damle, Nature (London), Phys. Sci. 241, 96 (1973).

[5]L. H. Smith, A. Buffington, G. F. Smoot, L. W. Alvarez, and M. A. Wahlig, Astrophys. J. 180, 987 (1973).

[6]A. Buffington, G. F. Smoot, L. H. Smith, and C. D. Orth, in *Proceedings of the Thirteenth International Conference on Cosmic Rays, Denver, Colorado, 1973* (University of Colorado, Denver, Colo., 1973), Vol. 1, p. 318.

[7]A. Buffington, C. D. Orth, and G. F. Smoot, "A Bremsstrahlung Identification Technique for Cosmic Ray Electrons and Positrons" (to be published).

[8]A complete description of our data analysis techniques is presented in Ref. 5.

[9]M. J. Ryan, J. F. Ormes, and V. K. Balasubrahmanyan, Phys. Rev. Lett. 28, 985 (1972).

[10]K. Pinkau, U. Pollvogt, W. K. H. Schmidt, and R. W. Huggett, in *Proceedings of the Eleventh International Conference on Cosmic Rays, Budapest, 1969,* edited by T. Gémesy *et al.* (Akademiai Kiado, Budapest, 1970), Vol. 1, p. 291.

[11]D. Müller and P. Meyer, Astrophys. J. 186, 841 (1973).

[12]J. L. Fanselow, R. C. Hartman, R. H. Hildebrand, and P. Meyer, Astrophys. J. 158, 771 (1969).

[13]J. K. Daugherty, Goddard Space Flight Center Report No. X-660-74-16, 1974 (to be published).

[14]B. Agrinier *et al.*, in *Proceedings of the Ninth International Conference on Cosmic Rays, London, 1965,* edited by A. C. Stickland (Institute of Physics and The Physical Society, London, 1966), Vol. 1, p. 331.

[15]K. C. Anand, R. R. Daniel, and S. A. Stephens, in *Proceedings of the Eleventh International Conference on Cosmic Rays, Budapest, 1969,* edited by T. Gémesy *et al.* (Akademiai Kiado, Budapest, 1970), Vol. 1, p. 235.

[16]R. Ramaty and R. E. Lingenfelter, Phys. Rev. Lett. 20, 120 (1968).

# Solving Equations of the Gell-Mann–Low and Callan-Symanzik Type

B. F. L. Ward
*Stanford University, Stanford, California 94305*
(Received 7 January 1974)

An examination is made of the dimensional analysis usually employed to solve the renormalization group equations for the asymptotic region. It is argued that if this analysis is done systematically, one must in general add new inhomogeneous terms to the asymptotic equations even after invoking Weinberg's theorem to discard the (generalized) mass insertion term. These new inhomogeneities are entirely determined by the physical thresholds of the theory. They are shown to provide a natural explanation of Bjorken scaling in interacting field theories.

Recently, some of the most exciting work[1] in the context of renormalizable quantum field theory has been done by employing the Gell-Mann–Low[2] and Callan-Symanzik[3] equations in the deep Euclidean region. These equations relate the responses of the one-particle irreducible (1PI) Green's functions of a renormalizable field theory to changes in the parameters of the theory. For example, in a theory with one field we have

$$[\mu\partial/\partial\mu+\beta(g)\partial/\partial g-n\gamma(g)]\Gamma_{\mathrm{asy}}^{(n)}=0, \tag{1}$$

where $\Gamma_{\mathrm{asy}}^{(n)}$ is the ultraviolet asymptotic part of the 1PI renormalized $n$-particle Green's function, $\beta$ and $\gamma$ are finite functions of the renormalized coupling constant $g$, and $\mu$ is the mass parameter of the theory, being either the renormalized mass or, for massless theories, the Euclidean renormalization point. Of course, in writing (1) for theories with masses, we are using Weinberg's theorem.[4]

Equation (1) provides, among other things, a convenient starting point for the discussion of Bjorken